DIRECT NUMERICAL SIMULATIONS OF COAXIAL JETS MIXING PROPERTIES

Guillaume Balarac, Mohamed Si-Ameur, Marcel Lesieur, Olivier Métais
MoST / L.E.G.I.,
B.P. 53
38041 Grenoble Cedex 09, France
guillaume.balarac@hmg.inpg.fr

ABSTRACT

Direct Numerical Simulations (DNS) are performed to study the mixing process in round coaxial jets. The mixing of the two fluids issued from the inner and annular streams is analysed by means of flow visualization and statistics of the mixing fraction field. It is shown that the annular ring structure has no influence on the mixing activity, when the annular stream and co-flow medium are seeded by the same chemical species. Nevertheless, a set of pure unmixed spots are observed, even in the far field, as the annular jet and the co-flow are seeded by two different species A and B. Analysis of the PDF and skewness of the scalar indicates that turbulent mixing process in the round co-axial jets acts intermittently through a radial periodic pulsation of the ring structures. The high level of the scalar dissipation has been observed to occur at the boundaries of the large turbulent structures.

INTRODUCTION

Coaxial jets are of great importance from the point view of fundamental research as well as industrial applications. The understanding of the global structure and of the turbulent mixing in coaxial jets helps for the design of new and efficient industrial devices (burners, injectors). A better fuel and oxidant turbulent mixing is of crucial importance to lead to higher combustion efficiency, lower pollutant emissions, and performance improvement of such devices. In this framework, the present work is focused on the study and analysis of turbulent scalar mixing in free coaxial jets. Free coaxial jets are made when the streams from the central and the co-annular pipes meet and mix in a open environment. Despite the fact that the flow originated by coaxial jets has been a topic of many numerical and laboratory experimental investigations (Salvetti *et al.*, 1996 and Rehab *et al.*, 1997), few research works available in the open literature have considered the important problem of mixing. The numerical investigations were limited to axisymmetric approximation (Salvetti *et al.*, 2000). It is well known on the basis of previous works dealing with simple configurations, e.g. homogeneous turbulence (Juneja and Pope, 1996; Li and Bilger, 1996), that turbulent mixing takes place at all turbulent scales. Typically, one speaks about a macro-mixing which is controlled by the turbulent structures. Thus, it is essential to understand, as a first step, the topology and detailed dynamics of such structures. This has been done in earlier works (da Silva *et al.*, 2003 and Balarac and Métais, 2005). One characteristic feature of coaxial jets is the existence of a recirculation bubble when the velocity ratio between the annular jet and the inner round jet is high enough.

The aim of the present work is to investigate mixing by means of Direct Numerical Simulation (DNS) in three-dimensional round coaxial jets. We restrict ourselves to mixing without chemical reaction by considering a passive scalar, in order to concentrate on the effect of the turbulent structures on the mixing process. In this context, a great attention has been paid to detailed evolution of the spatial and temporal evolution of the mixing fraction, f, while benefiting from the advantage of the spatially developing approach. Even though the present DNS is restricted to low Reynolds number (in order to resolve all the turbulent mixing scales), it can be considered as a noteworthy step for our under-development work at high Reynolds number. A nearly fully developed flow has been reached in far field (as shown by the flow dynamic field), which give confidence to track the mixing process within a strong stirring conditions. Therefore the objective of the present investigation is to provide a numerical description (by means of visualization of snapshots of the flow and of statistics based on temporal and spatial informations) of the mixing mechanism between two passive species A (e.g Air) an B (e.g Fuel) seeded in the coaxial jets.

NUMERICAL METHOD

Since the DNS is the tool of investigation, the full incompressible Navier-Stokes equations written in Cartesian coordinates have been solved numerically in a parallelepipedic computational domain. The spatial discretization is performed by a sixth-order compact finite difference scheme in the streamwise direction, together with pseudo-spectral methods in transverse and spanwise direction. Pressure-velocity coupling is assured by a fractional step method, requiring solving a Poisson equation to insure incompressibility of the velocity field. The advancement in time is carried out by a third order Runge-Kutta scheme. The outlet boundary condition is of a non-reflective type. Full numerical discretization details can be found in da Silva and Métais (2002). A focus on the evolution of a mixing in near and far field, a transport equation (convection-diffusion) for the mixing fraction is solved simultaneously with the flow equations. For the spatial discretization of the convection term, we used a second-order semi-discretized TVD Roe scheme (Hirsch, 2002).

The shape of the inlet velocity profile is constructed with two 'hyperbolic tangent' profile. In addition, we superimpose a random noise on the inlet profile. This noise is applied on the three velocity components with a weak amplitude (see da Silva *et al.*, 2003 for details). In this work, we investigate two values of the velocity ratio: $r_u = 5$ (case without recirculation bubble) and $r_u = 17$ (case with recirculation bubble). All simulations are carried out on the same grid

which consists in $231 \times 384 \times 384$ points and allows a domain size of $10.8D_1 \times 10.65D_1 \times 10.65D_1$, along the streamwise ($x$) and the two transverse directions (y, z), respectively. The Reynolds number is $Re = U_2 D_1/\nu = 3000$ and the diameter ratio is $\beta = D_2/D_1 = 2$. The mixing scalar, f, is equal to one initially in the annular jet or in the central jet (and $f = 0$ elsewhere). The Schmidt number is taken equal to one. To our knowledge, this is the first DNS dealing with mixing in round coaxial jets.

RESULTS AND DISCUSSION

In order to focus our analysis and discussions on the scalar dispersion (mainly turbulent mixing), as it is strongly linked to combustion systems, we assume that the mixing is due to two chemical species A (air) and B (fuel). Two cases are considered in the present work, regarding the species B (fuel) seeded initially in the fast annular stream or the slow central stream, and A (air) seeded in the ambient medium and the stream without fuel. The A-B mixing is tracked through the spatial and temporal evolution of the mixing fraction f. The results are analysed with a various statistics and illustrations based on visualizations of a number of snapshots and animations.

Flow Dynamics

First, flow dynamic is studied before dealing with mixing properties. Figure 1 shows isosurfaces of positive Q for a coaxial jet. We recall that Q is the second invariant of the velocity gradient tensor and is a good way to identify the flow coherent vortices (Hunt *et al.*, 1988). The main features of the flows can be seem here. First, primary vortices develop on both shear layers (between the inner and the outer jets and between the outer jet and the co-flow). These vortices are due to Kelvin-Helmholtz instability created by the shape of the upstream velocity profile. In the case of coaxial jet with high velocity ratio ($r_u > 1$), the inner primary vortices are trapped between two consecutive outer vortices. Thus, there is a "locking" phenomenon between the outer and inner vortices (Balarac and Métais, 2004). Around $x/D_1 \approx 7$, pairs of streamwise vortices appear between two consecutive outer or inner primary vortices, stretched in the stagnation regions between them. The streamwise vortices play a dominant role in the transition processes towards a fully turbulent state. Moreover, the location where the streamwise vortices appear is very dependent of the inlet conditions (Balarac and Métais, 2005). The emergence of the streamwise vortices is soon followed by an abrupt increase in the level of small scale turbulence, and the flow reaches quickly a state of fully developed turbulence. Thus, the time spectrum computed from the axial velocity component at the end of the computational domain has a $-5/3$ range over about one decade followed by a smooth transition into the dissipative region (figure 2 *(b)*).

Figure 2 *(a)* shows the axial velocity profile at several positions. At the beginning of the transition, the coaxial jet keeps a profile similar to the initial profile. But downstream of $x/D_1 \approx 8$, the axial velocity profile is closer to a single round jet profile: the profile has lost its two-layer structure and the maximum velocity is located at the centerline. The fully turbulent state of a coaxial jet is comparable with the fully turbulent state of a single round jet with an initial velocity U_2 and diameter D_2 (Ko and Kwan, 1976). Thus, there is a strong momentum transfer from the annular jet to the central jet. This phenomenon carries out a "pinching" of the central jet by the annular jet (Rehab *et al.*, 1997) and plays a role on the mixing (Suzuki, 2000).

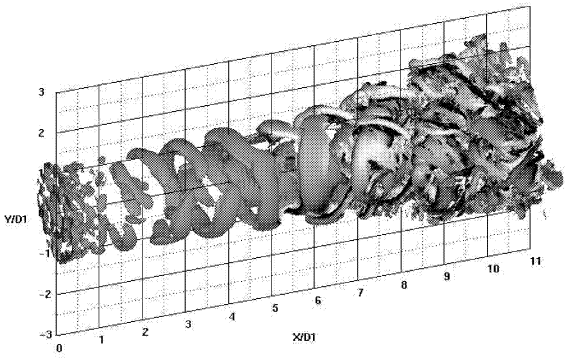

Figure 1: Isosurface of positive Q coloured by the axial vorticity to show the streamwise vortices (black and white).

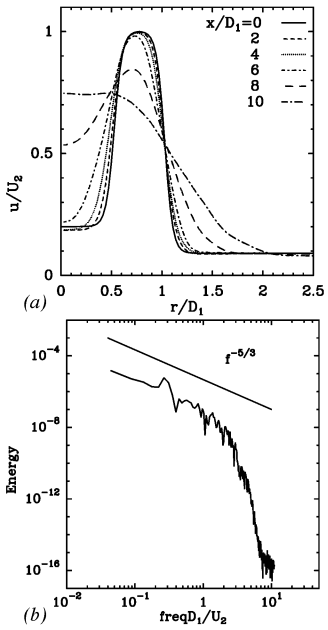

Figure 2: *(a)* Axial velocity profile at several sections. *(b)* Frequency spectrum of the axial velocity signal at $x/D_1 \approx 10$.

Finally, when the velocity ratio exceeds a critical value, a recirculation bubble appears near the entrance of the jet (Rehab *et al.*, 1997 and da Silva *et al.*, 2003). When r_u increases, the entrainment by the outer annular jet is more and more pronounced and requires the return of the downstream fluid (figure 3). Note that there is a strong interaction between this bubble and the surrounding flow (Balarac and Métais, 2005).

First case: species B seeded in the annular jet

We prescribe an inlet mass fraction profile which ensures a value of $f = 1$ for a pure species B in the annular stream and $f = 0$ for pure air elsewhere (inner jet and co-flow). To qualitatively illustrate mixing, the instantaneous planar flow visualization along the central plane is shown in figure 4. We can observe the near field (first region) which is quasi-linear

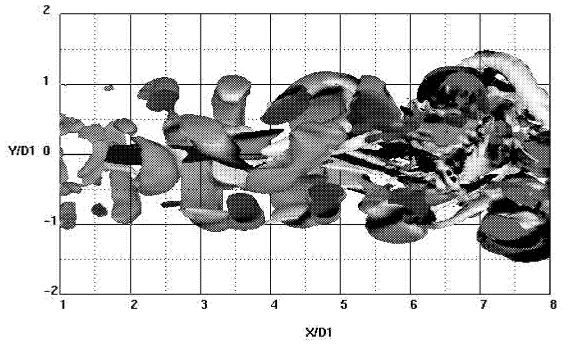

Figure 3: Cut view of positive Q isosurface coloured by the axial vorticity. The recirculation bubble is in the center of the jet.

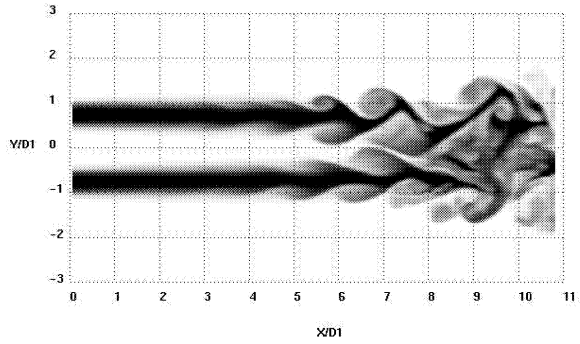

Figure 4: Instantaneous contours of mixing fraction in the central plane. f varies from 0 (white) to 1 (black).

until $x/D_1 = 5$. Note that the extension of this region is important because of the nature of the perturbation (white noise) introduced at the inflow which is of weak amplitude (roughly 3% of the fast annular stream) and thus allows the instabilities to develop naturally. However, discrepancies with the experimental measurements are systematic in this region as it depends strongly on the inlet condition. The mass exchange between the annular and inner streams is mainly dominated by molecular diffusion in the near field. This observation is also supported by statistics, especially the mean mixing fraction profiles (figure 5). For $x/D_1 < 5$, one can observe on the axial development of the mean centerline (both inner and annular streams) mixing fraction profiles, that the values of f remain equal to 1 and 0 respectively. On the contrary, the radial mean mixing fraction profiles at various downstream positions indicate clearly for $x/D_1 < 5$ a variation of f at the interface between the two species A and B. This variation is due to molecular diffusion which mix A and B in the radial direction. Beyond $x/D_1 = 5$, the entrainment of the fluid species into the shear layers improves the mixing activity. Along the centreline for both the inner and outer jets, the mean mixing fraction decays and increases respectively, to reach an asymptotic value around $f = 0.5$. Thus, the A-B species in the heart of the rings structure of the inner and outer jets are in equal-partition mixing and reasonably uniformly distributed. One can note that the longitudinal gradients of the mean centreline mixing fraction for both the inner and annular streams are uneven. Hence, the amounts of mass of species A and B

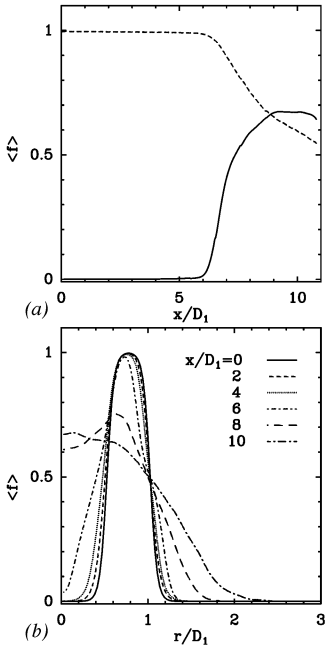

Figure 5: Mean mixing fraction. *(a)* Downstream evolution in both central (continuous line) and annular jet (dashed line). *(b)* Radial evolution at several downstream locations.

entrained inside the shear layers are asymmetric. As it is quantitatively evident below, the A species issued from the central jet remain confined between the edge (of the inner jet) and the centreline. The A-B mixing near the heart of outer rings which ensures a value of about 0.5 is essentially composed of species A issued from the ambient co-flow and species B issued from the outer flow.

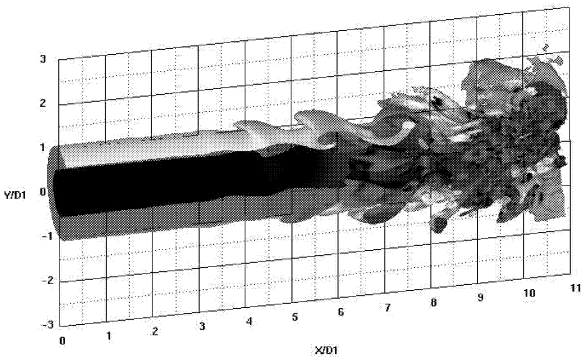

Figure 6: Cut view of isosurface of mixing fraction ($f = 0.5$) coloured by the tangential vorticity.

Figure 6 shows iso-mixing fraction surface $f = 0.5$ which is a good indicator of the mixing efficiency in the turbulent mixing conditions. Characterization of the multiscale geometry of the iso-species surfaces is a crucial step for understanding and modeling turbulent mixing linked to turbulent combustion processes. The isosurface $f = 0.5$ is highly convoluted after the amplification of the instabilities, with evidence of a large scale structure. In figure 6, the isosurface is coloured by the tangential vorticity field, one can distinguish two noticeable geometries fulfilling $f = 0.5$. Before the transition regime $x/D_1 < 5$, the two structures are wholly decorrelated, while

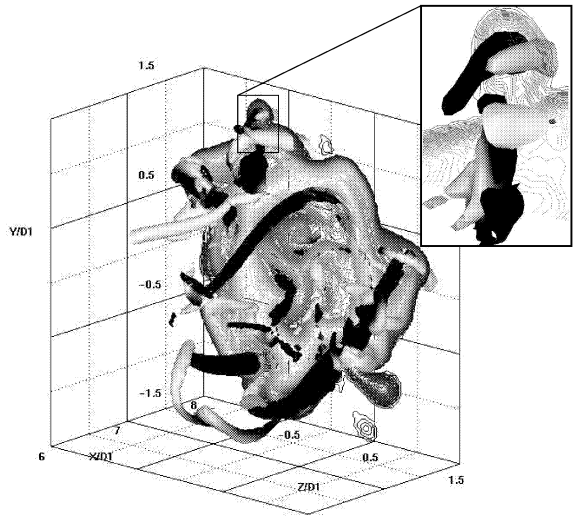

Figure 7: Illustration of the passive scalar ejections by the contrarotating longitudinal vortices (shown by an isosurface of $Q > 0$ and coloured in black or white).

for $x/D_1 > 5$ they are strongly distorted which allows interpenetration between the two species A and B. Instantaneous animations of isosurface $f = 0.5$ and planar visualization in $y-z$ plane cut shows the crucial role played by the contrarotating longitudinal vortices to eject the species B intermittently, into the ambient fluid (figure 7) and the inner jet. An exhaustive observation of the animations reveals that the intermittent specificity of the turbulent mixing process combines a radial periodic pulsation of the ring structures with the longitudinal contra-rotating structures. The periodic pulsation induces a radius variation (bounded by the maximal and minimal shear radius) of the rings, and subsequently alter the action of the mushroom structure to eject species B into the edge of the surrounding streams made up of species A. Moreover, as it is evident on figure 4, large amounts of unmixed species B persist as spots even far downstream where stirring conditions are strong and the diffusion interface is enlarged. An appropriate frequency forcing of 3D longitudinal structures as well as of vortical rings at the inlet boundary could decrease the amount of pure species.

Figure 5 *(b)* shows the radial profiles of the mean mixing fraction at various downstream positions. For $x/D_1 > 5$, the A-B mixing spreads out in the radial direction, as far as the axial position increases, and hence expands the jet width. In fact, the radial spreading rate of the A-B mixing is sustained by the large turbulent structures which generate large convoluted front of mixing submitted to strong stirring conditions. Further examination of the radial profiles reveals that the evolution of mean mixing fraction is quasi-Gaussian, when the radial position is scaled by the axial position. The rms of the mixing fraction fluctuation is shown in figure 8. The radial profiles at various axial positions indicate that the turbulent mixing becomes important for $x/D_1 > 5$. Two distinct peaks are obviously perceptible, located respectively within the hearts of the ring structures issued respectively from the inner and outer jets. Thus, the two peaks are the signatures of the large structures that occur in the inner and outer streams. Near the outflow, merely the outer peak persists as a consequence of prevalence of outer jet mixing properties. This

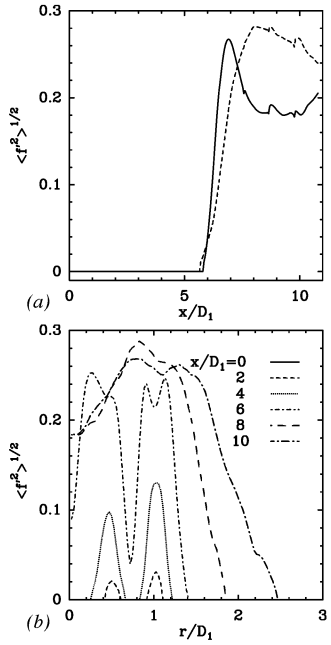

Figure 8: The rms of the mixing fraction. *(a)* Downstream evolution in both central (continuous line) and annular jet (dashed line). *(b)* Radial evolution at several downstream locations.

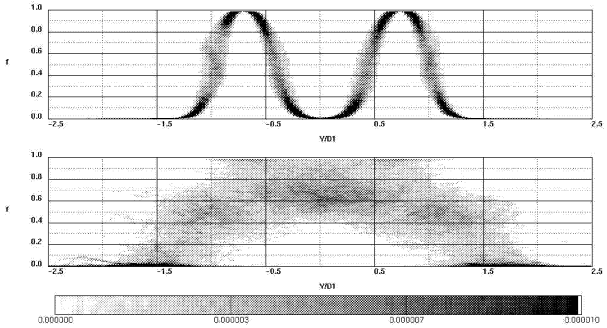

Figure 9: Radial profiles of the PDF at $x/D_1 = 5$ (top) and $x/D_1 = 10$ (bottom).

observation is confirmed by figure 9. It shows the radial profiles of the PDF at various axial positions. One can note the presence of largely mixing zones which enlarge the flow thickness', especially beyond $x/D_1 > 5$. Near the outflow position, the inner and outer mixing merge in order to create a single mixing zone similar to simple jet. Moreover, these PDF show an important intermittency in the mixing zones: for $x/D_1 < 5$, it is in both mixing zone (Figure 9 top) and after $x/D_1 \approx 6$, it is in the single mixing zone created (Figure 9 bottom). Figure 10 shows the radial profiles of the skewness of the mixing fraction at various downstream positions. It corroborates this point. Indeed, the scalar skewness exhibits two decrease-increase variations close to the intermittency of the behavior of the mixing at the edges of the inner and outer rings when $x/D_1 \approx 6$. After, there is an increase variation at the single mixing zone at the end of the jet.

Figure 11 shows the instantaneous scalar dissipation field, whose analysis is of great importance for scalar subgrid mod-

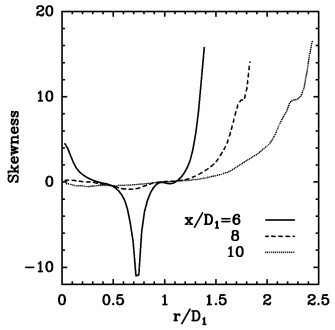

Figure 10: Radial profiles of the mixing fraction skewness at several downstream locations.

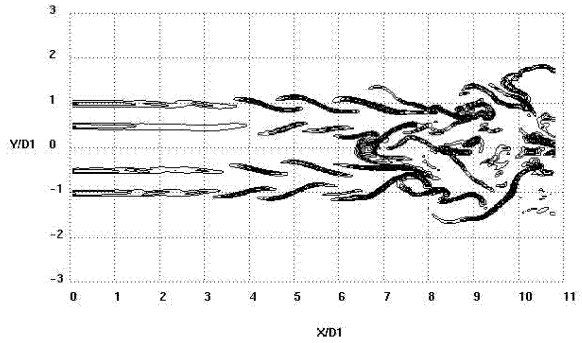

Figure 11: Instantaneous scalar dissipation field in the central plane.

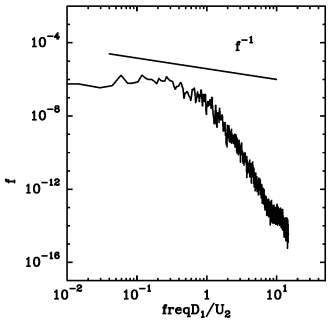

Figure 12: Frequency spectrum of the fluctuation of the mixing fraction at $x/D_1 \approx 10$.

eling in large eddy simulations of reacting flows. The intense scalar dissipation regions have sheet-like structures and occur at the boundaries of the large turbulent structures. This explains the cascade of scalar dissipation (figure 12) through a well-defined inertial-convective scaling range, similarly to energy spectra, but with a slope between $-5/3$ and -1. This result shows the contrast between the velocity and the scalar fields, even at Schmidt number $Sc = 1$ (see Lesieur and Rogallo (1989) in isotropic turbulence).

Finally, Figure 13 shows an instantaneous planar flow visualization along the central plane for a coaxial jet with a recirculation bubble ($r_u = 17$). The bubble allows fuel invasion in the central jet as of the beginning of the jet. It is largely favorable to the mixing in the first stage of the transition. And it allows to find a more important mixing zone at the end of the jet.

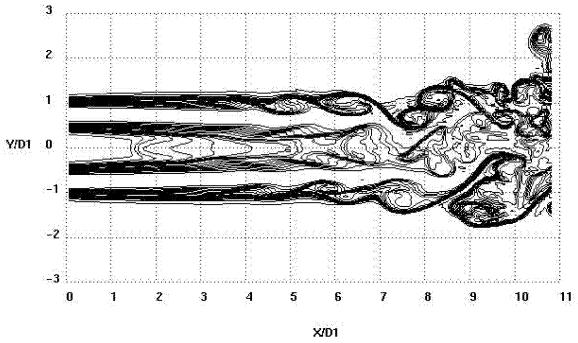

Figure 13: Instantaneous contours of mixing fraction in the central plane for a coaxial jet with a recirculation bubble ($r_u = 17$).

Second case: species B seeded in the central jet

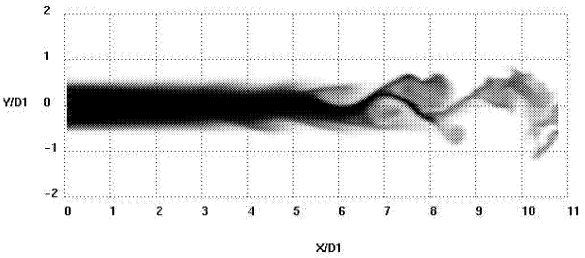

Figure 14: Instantaneous contours of mixing fraction in the central plane. f varies from 0 (white) to 1 (black).

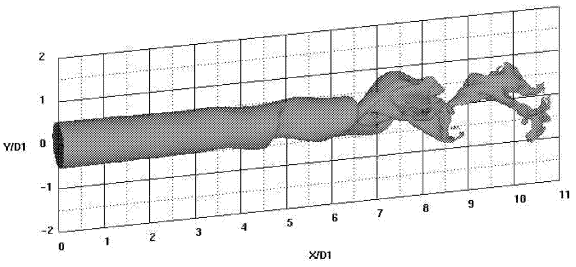

Figure 15: Isosurface of mixing fraction ($f = 0.5$) colored by the tangential vorticity.

Now, we impose an inlet mass fraction profile with $f = 1$ for a pure species B in the inner stream and $f = 0$ for pure air elsewhere (annular jet and co-flow). An analyse of the snapshots of scalar field visualizations (figure 14) reveales that the mixing activity is utterly confined in the inner jet and its periphery. Beyond $x/D_1 = 7$, an interesting upshot as regards the absence of pure unmixed species is obviously noticeable. Thus, the unmixed spots observed in the previous case are mainly due to outer and co-flow streams. Improving mixing efficiency suggests therefore to act only on the outer jet by a suitable frequency forcing. The isosurface $f = 0.5$ (figure 15) is highly convoluted near the edge of the inner and outer streams, a noteworthy difference with the previous case perceptible in particularly by looking at the volumetric aspect and the width of the large scale structures.

Similarly to the preceding case, an instantaneous animations of isoscalar $f = 0.5$ and planar visualization in y-z plane

cuts have been carried out. Mushroom shaped contrarotating longitudinal structures do eject species intermittently inside the rings structure. The same mechanism of the turbulent mixing described previously is observed. However, one can note that the radial pulsation is more important and its contributes to confine the scalar in the inner jet.

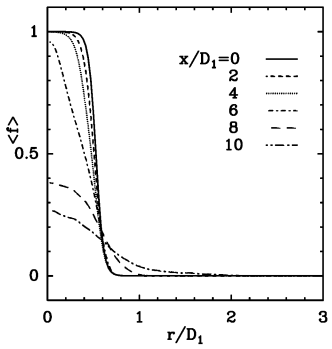

Figure 16: Radial profiles of the mean mixing fraction at several downstream locations.

The confinement of the mixing activity inside the inner jet is also supported by statistics. Indeed, the radial mean mixing fraction profiles at various axial positions (figure 16) indicate evidently that the maximum variations of f occur inside the inlet curve between $0 < r/D_1 < 1$. This interval corresponds to the edge of inner jet, and one can observe that the mixing in front of the periphery is less important than within the inner jet. Therefore, on the basis of snapshots animations and statistics, one can underline that the species B issued from the inner jet remain captured between the centreline the edge of the central stream. On the other hand, the species A of the central jet reach the centreline of the inner jet to mix with species B, as it is indicated by the decreasing of the mixing fractions from 1 to an intermediate value (indicative of the local mixing).

CONCLUSIONS

We have performed a qualitative and quantitative investigation of the mixing process in round coaxial jets by means of Direct Numerical Simulations. The mixing of two passive species A (e.g air) and B (e.g fuel) has been tracked through the spatial and temporal evolution of the mixing fraction. The spatially developing approach has allowed to observe the mixing process phases until a sufficient stirring conditions, although our computations are carried out at low Reynolds number. The above analysis has highlighted significant results. The fluid issued from the central jet remains confined between the edge of the inner jet and the centreline, whereas the other fluid issued from the annular jet reaches all the space of the central jet inducing an A-B mixing without pure unmixed spots. This result has an important the industrial applications. Indeed, the seeding of the inner jet by species B (e.g fuel) and elsewhere by species A (e.g air) induces a segregation of the annular shear layer to participate to the mixing process. In other hand and in spite of the fact that the annular turbulent rings and their mushrooms structures are dynamically highly active, a great contrast between the width of the jet and the mixing zone has been observed, which show the impossibility for these structures to bring mass species from the inner jet. However, a set of spots of pure unmixed species has been observed in the first case, which may represent a disadvantage for the mixing efficiency. These spots are exclusively due to the annular shear layer, as demonstrated by the comparison between the two cases. This result suggests then to act wholly on the annular jet by an appropriate frequency forcing. Snapshots visualizations of snapshots and statistics (PDF, Skewness) of the flow have shown that the turbulent mixing process in the round coaxial jets acts intermittently through a radial periodic pulsation of the ring structures and then limit the efficiency of the longitudinal mushroom structures.

Further investigations at high Reynolds numbers are undertaken based on LES approach, especially to analyse the important open problem of effect of the Reynolds number on the scalar field.

REFERENCES

Balarac, G., and Métais, O., 2004, "Coherent vortices in coaxial jets", *Advances in Turbulence X*, H. I. Anderson and P.-Å. Krogstad ed., CIMNE, pp. 149-152.

Balarac, G., and Métais, O., 2005, "The near field of coaxial jets: a numerical study", *Phys. Fluids*, accepted.

Hirsch, C., 2002, "Numerical Computation of Internal and External Flows, Vol. 2", Wiley, John & Sons.

Hunt, J. C. R., Wray, A. A., and Moin, P., 1988, "Eddies, stream, and convergence zones in turbulent flows", Annual research briefs, Center for Turbulence Research, Stanford.

Juneja, A., and Pope, S. B., 1996, "A DNS study of turbulent mixing of two passive scalars", *Phys. Fluids*, Vol. 8, pp. 2161-2184

Ko, N. W. M., and Kwan, A. S. H., 1976, "The initial region of subsonic coaxial jets", *J. Fluid Mech.*, Vol. 73, pp. 305-332.

Lesieur, M., and Rogallo, R., 1989, "Large-eddy simulation of passive scalar diffusion in isotropic turbulence", *Phys. Fluids A*, Vol. 1, pp. 718-722.

Li, J. D., and Bilger, R. W., 1996, "The diffusion of conserved and reactive scalars behind line sources in homogenous turbulence", *J. Fluid Mech.*, Vol. 318, pp. 339-372.

Rehab, H., Villermaux, E., and Hopfinger, E. J., 1997, "Flow regimes of large-velocity-ratio coaxial jets", *J. Fluid Mech.*, Vol. 345, pp. 357-381.

Salvetti, M. V., Orlandi, P., and Verzicco, R., 1996, "Numerical simulations of transitional axisymmetric coaxial jets", *AIAA Journal*, Vol. 34, pp. 736-743.

Salvetti, M. V., Orlandi, P., and Verzicco, R., 2000, "Effects of velocity ratio on vorticity dynamics and mixing in coaxial jet flow", *1st International congress in Turbulent Shear Flows Phenomena.*

da Silva, C. B., Balarac, G., and Métais, O., 2003, "Transition in high velocity ratio coaxial jets analysed from direct numerical simulations", *J. of Turbulence*, Vol. 4, 24.

da Silva, C. B., and Métais, O., 2002, "Vortex control of bifurcating jets: a numerical study", *Phys. Fluids*, Vol. 14, pp. 3798-3819.

Suzuki, Y., Kasagi, N., Horiuchi, Y., and Nagoya, D., 2000, "Synthesized mixing process in an actively-controlled confined coaxial jet", *4th JSME-KSME Thermal Engineering Conference.*